Macrothink Institute™

Environmental Management and Sustainable Development
ISSN 2164-7682
2024, Vol. 13, No. 1

Effects of Landscape Fragmentation on Soil Loss in the Cerrado Biome, Brazil

Ana Paula Camelo (Corresponding author)

Dept. of Forestry Engineering, University of Brasilia

Asa Norte, Campus Darcy Ribeiro, Brasília, DF, Brazil

E-mail: paulaflorestal@gmail.com

Keila Sanches

Federal Institute of Brasília, Campus Samambaia, Brasília, DF, Brazil

E-mail: keila.sanches@ifb.edu.br

Eraldo Aparecido Trondoli Matricardi (Corresponding author)

Dept. of Forestry Engineering, University of Brasilia

Asa Norte, Campus Darcy Ribeiro, Brasília, DF, Brazil

E-mail: ematricardi@gmail.com

Edson Eyji Sano

Brazilian Agricultural Research Corporation (Embrapa Cerrados)

PO Box 08223, Planaltina, DF, Brazil

E-mail: edson.sano@embrapa.br

Álvaro Nogueira de Souza

Dept. of Forestry Engineering, University of Brasilia

Asa Norte, Campus Darcy Ribeiro, Brasília, DF, Brazil

E-mail: ansouza@unb.br

Macrothink Institute™

Environmental Management and Sustainable Development
ISSN 2164-7682
2024, Vol. 13, No. 1

Eder Pereira Miguel

Dept. of Forestry Engineering, University of Brasilia

Asa Norte, Campus Darcy Ribeiro, Brasília, DF, Brazil

E-mail: migueleder pereira@gmail.com

Received: September 5, 2023 Accepted: March 6, 2024 Published: March 14, 2024

doi:10.5296/emsd.v13i1.21288 URL: https://doi.org/10.5296/emsd.v13i1.21288

Abstract

Soil loss stands as a critical global challenge, posing economic and environmental threats to soil and water conservation. This study aimed to assess the impact of landscape changes on soil loss in the Descoberto River basin, encompassing 62 watersheds in the Cerrado biome in central Brazil. We analysed a 32-year time series (1985–2017) of land use and land cover data based on geostatistical techniques and spatiotemporal weighted regression analysis. Principal component analysis condensed 16 landscape metrics into three factors: aggregation/diversity, dispersion/adjacency, and patchiness. The average annual total soil loss across all 62 analysed watersheds was estimated at 73.3 ± 78.2 (standard deviation) ton ha^{-1}. A significant positive correlation was observed between landscape fragmentation and soil erosion, indicating that, as fragmentation increases, soil losses also increase. Furthermore, our analysis revealed a decreasing trend in soil loss rates in recent years, primarily attributed to the recovery of native vegetation since no significant soil management practices were widely implemented in the study area during the study period.

Keywords: Brazilian Savannah, Landscape, Erosion, Discretized and spatial-temporal models

1. Introduction

Soil erosion is an important global issue due to its negative impacts on soil productivity, nutrient loss, siltation in water bodies, and degradation of water quality (Benavidez et al., 2018). The projected global annual potential soil erosion rate, by 2012, averaged 2.4 ton ha^{-1}. In tropical regions like the Cerrado biome, this rate is expected to increase between 30% and 50% by 2070 under climate change scenarios (Borrelli et al., 2020; Wuepper et al., 2020).

The Cerrado biome has become the main agricultural frontier in Brazil, driven by factors such as its flat topography, infrastructure, and low land prices (Garcia et al., 2017; Garrett et al., 2018). However, land occupation has led to landscape fragmentation by reducing and isolating natural habitats. Urbanization of natural areas is a major cause of soil erosion (Trabaquini et al., 2017; Ledda and Montis, 2019; Queiroz et al., 2020).

Land use and land cover (LULC) changes in Brazil are dynamic and spatially dependent

(Soares-Filho et al., 2013; Jusys, 2016). Soil erosion has gained global environmental and social concern due to the overall increase in LULC changes in recent decades, necessitating a better understanding of its location and magnitude at various scales and time periods (Borrelli et al., 2020; Hurtt et al., 2020). It is also crucial to comprehend the factors influencing soil erosion across multiple spatial-temporal scales (Ouyang et al., 2010; Qi et al., 2012; Mitchell et al., 2015; Hu et al., 2019).

Original erosion models utilizing remotely sensed data and geographic information systems (GIS) have been employed to assess soil erosion rates and to map LULC changes at local, regional, and global scales using multitemporal datasets (Bera, 2017; Tadesse et al., 2017). However, the spatial heterogeneity of the erosion process poses limitations on these models (Gao and Wang, 2019).

The Geographically weighted regression (GWR), proposed by Fotheringham et al. (2002), addresses this limitation effectively. However, the GWR does not account for temporal non-stationarity, which is also a significant factor influencing land use changes (Ma et al., 2018). Huang et al. (2010) proposed geographically and temporally weighted regression (GTWR), which has proven to be a robust technique for capturing spatial and temporal non-stationarity simultaneously, thereby enhancing environmental models considerably (Ma et al., 2018; Cui et al., 2019). While there are limitations in soil loss prediction models, the task remains challenging in most developing countries due to scarce monitoring systems related to social, economic, and political changes (Hrachowitz et al., 2013).

In this study, we investigated the effects of land use changes and landscape fragmentation on soil loss in the Descoberto River basin, located in the Cerrado biome, Brazil. This region is pivotal in supplying most of the potable water to the population of the Federal District, Brazil. Our findings indicate a distinct relationship between landscape fragmentation and soil erosion. The results of this study have great potential to contribute to the formulation of public policies aimed at enforcing effective land use and soil management practices to mitigate the impacts of land use changes and landscape fragmentation on soil loss in the study region.

2. Method

2.1 Regional Setting: Central Brazilian Cerrado Biome

Our study focused on the upstream region of the Descoberto River basin, covering a total of 356.73 km² in the western Federal District of Brazil (Figure 1). More than 50% of native vegetation in the study area has been converted into agricultural lands, forest plantations, and urban areas over recent decades (Nunes and Roig, 2016). The Descoberto River basin is of socio-environmental significance, as it supplies 66% of the water to the Federal District of Brazil for domestic and agricultural consumption, including Brasília and surrounding satellite cities (Ferreira et al., 2015).

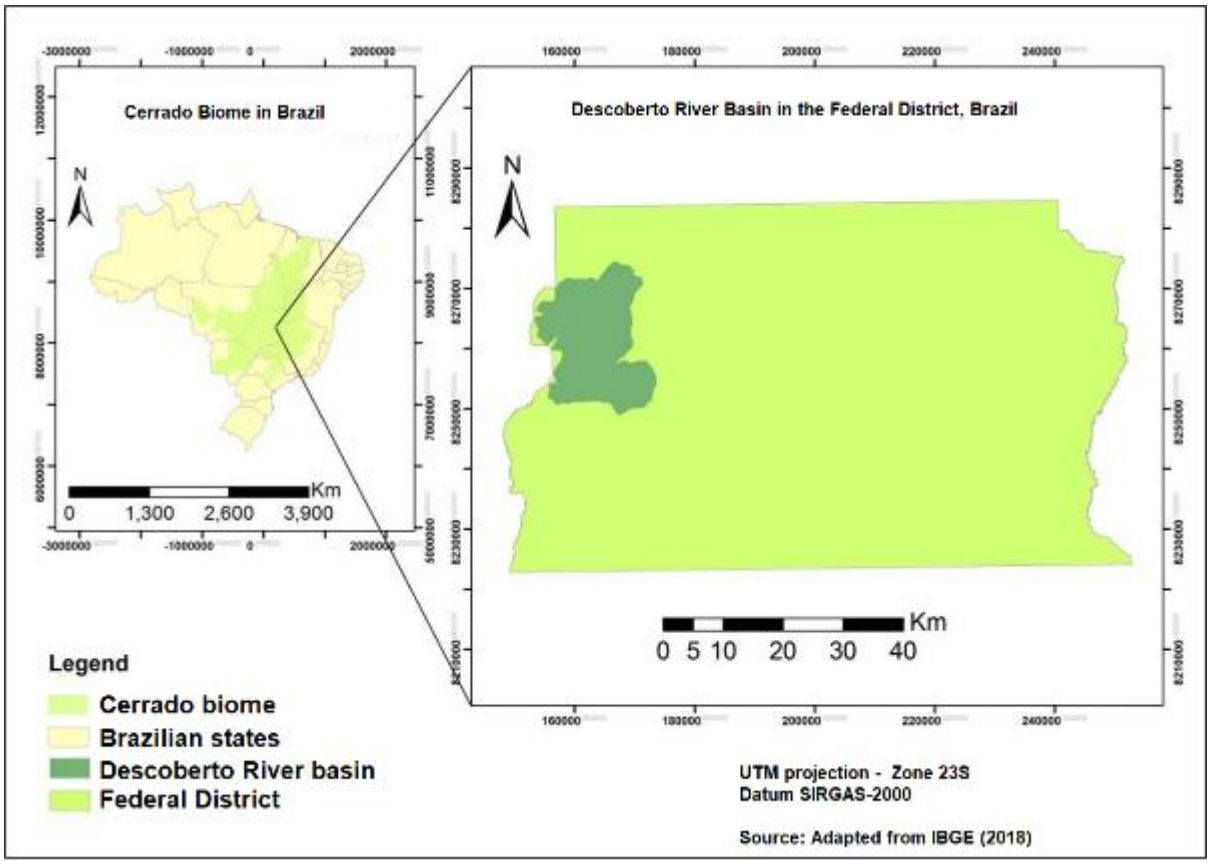

Figure 1. Location of the study area, which encompasses the Descoberto River basin, within the Federal District of Brazil

In the Descoberto River basin, the most prevalent soil classes are Red Latosols and Red-Yellow Latosols. However, other soil classes, including Nitosols, Haplic Cambisols, Haplic Gleysols, Petroplinthic Ultisols, Quartzipsamments, and Spodosols, are also present (Reatto et al., 2003). The altitude in the study area ranges from 1000 m to 1343 m, and it features a predominantly Cwa-type climate according to the Köppen climate classification. This climate is characterized by dry winters and hot humid summers, as documented by CODEPLAN (2020). The average annual precipitation in the region varies between 1200 mm and 1750 mm (Nunes and Roig, 2016).

2.2 Land Use and Land Cover Dataset

The LULC dataset for this study was sourced from the MapBiomas project (MapBiomas, 2018a), collection 3.0, providing a 30-meter spatial resolution data for the period between 1985 and 2017. The overall accuracy of the MapBiomas dataset is reported as 84%. However, to improve this accuracy, corrections were implemented using higher-resolution images available in the Google Earth platform (Schwieder et al., 2016; Kassawmar et al., 2018).

Urban area boundaries also underwent refinement and reclassification based on the Federal District Urban Evolution database. This database utilized 1-meter spatial resolution

orthophoto mosaics covering the period from 1958 to 2015 (SEDUH, 2019).

Additionally, the original 21 LULC classes were reclassified into six broader categories, namely natural forest formation, savanna/grassland formation, planted forest, agricultural fields, water bodies, and urban areas. This reclassification aligns with the MapBiomas General Handbook (MapBiomas, 2018b).

2.3 Digital Elevation Model and Area Discretization

The boundary of the Descoberto River basin was delineated using the ArcHydro function available in the ArcGIS® 10.8 software. To generate the digital elevation model (DEM) required for this analysis, we utilized the Shuttle Radar Topography Mission (SRTM) data provided by the National Aeronautics and Space Administration (NASA) at a spatial resolution of 30 meters (NASA, 2023).

2.4 Watershed Delimitation

Spatial discretization forms the fundamental basis for all simulations involving spatial distribution, as highlighted by Liao et al. (2020). In this research, we focused on a collection of watersheds situated within the Descoberto River basin, aiming to assess the influence of LULC changes on soil erosion within each specific watershed. To achieve this, we utilized an automated watershed delimitation technique, which enabled the division of the entire Descoberto River basin into 62 distinct individual watersheds.

2.5 Universal Soil Loss Equation (USLE)

To estimate soil loss in the study area, we applied the Universal Soil Loss Equation (USLE), originally proposed by Wischmeier and Smith (1978). The USLE is represented by the following equation:

$$A = R * K * LS * CP \quad (1)$$

Where: A = the predicted long-term average annual soil loss (ton ha^{-1} year^{-1}); R = the rainfall and runoff erosivity factors (MJ mm ha^{-1} h^{-1} year^{-1}); K = the soil erodibility factor (tons ha^{-1}); L= the slope length factor (dimensionless); S = the slope steepness factor (dimensionless); C = the crop management factor (dimensionless); and P = the supporting practices factor (dimensionless). In this analysis, the C and P factors were combined to create the CP factor, assuming that no significant soil erosion control practices have been widely implemented in the study area and, therefore, CP = 1.

The R factor was calculated based on the monthly average erosion index (EI), as shown in Eq. 2, which has been widely used for this purpose (Bertoni and Lombardi Neto, 1999). In this analysis, the R factor was estimated by adding the monthly values of the soil erosion indices, as expressed in Equations 2 and 3.

$$EI = 67.355 \times \left(\frac{r^2}{P}\right)^{0.56} \quad (2)$$

$$R = \sum_{i=1}^{12} EI \quad (3)$$

Where: *EI* = the monthly average erosion index (MJ mm ha^{-1} h^{-1}); *r* = the average monthly precipitation (mm); and *P* = the average annual precipitation (mm).

A dataset comprising 32 years of daily rainfall data was acquired from three meteorological stations located within or near the Descoberto River basin. These stations are named Brazlândia (World Meteorological Organization ID: 1548007), Descoberto (ID: 1548008), and Taguatinga (ID: 1548006) stations (Figure 2). To spatially represent rainfall across the study area, we utilized the inverse distance weighted (IDW) interpolation technique. The IDW default setup was applied, which involves calculating the weighted average of rainfall from the *n* nearest neighbors (Tiwari et al., 2019). The annual rainfall trend in the dataset was assessed using the Mann-Kendall test (Nyikadzino et al., 2020).

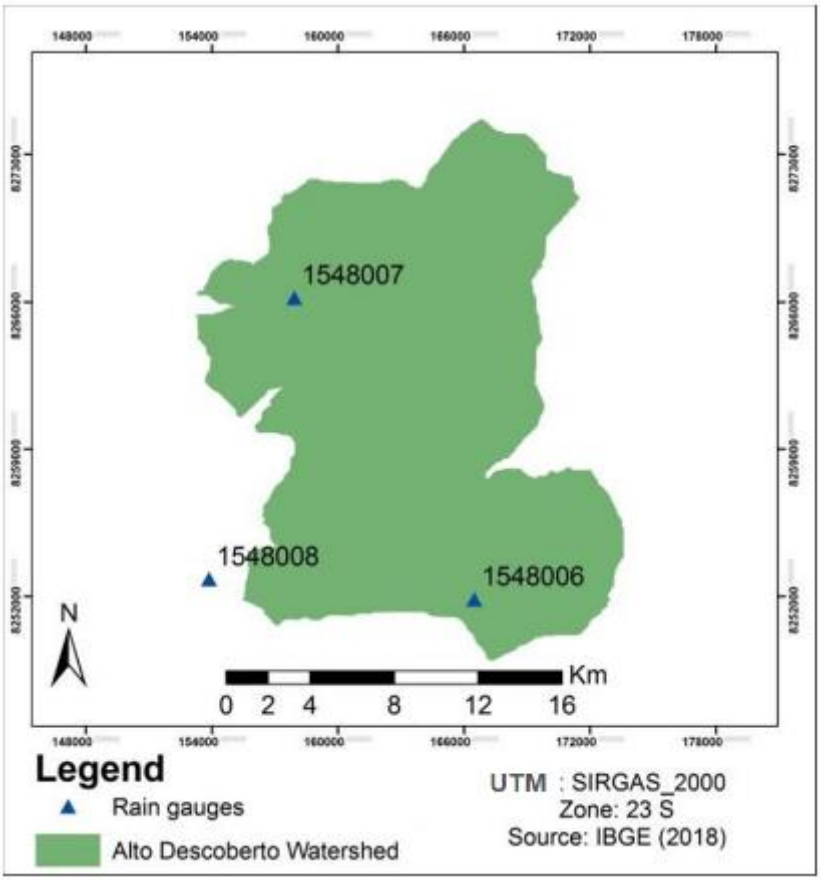

Figure 2. Location of the meteorological stations in the Descoberto River basin and in the surrounding areas

The *K* factor is defined as the rate of soil loss per unit of the rainfall erosion index (*R*) and is measured on a specific plot (Wischmeier and Mannering, 1969). In our study area, we utilized the *K* values developed and tested by Mannigel et al. (2002), Reatto et al. (2003), and Silva and Alvares (2007) for each soil type.

To compute the *LS* factor, we employed the ArcHydro and ArcGIS raster calculator tools,

using the following equation:

$$LS = \left(\frac{FA \times grid\ size}{22.13}\right)^{0.4} \times \left(\frac{s}{0.0896}\right)^{1.3} \quad (4)$$

Where: *FA* = the flow accumulation; *grid size* = the size of a cell side of the DEM data (30 m) used in this analysis; and *S* = the sine of the slope angle.

The *C* factor is influenced by the land use characteristics of a specific basin or watershed, while *P* factor values are assigned based on cultivation methods (Wischmeier and Mannering, 1969). In our study, the land use map of the study area was reclassified based on *CP* factor values developed and tested by Wischmeier and Smith (1978) and Lopes et al. (2009)..

As previously described, Equation 1 provides the average annual soil loss in tons per hectare per year for each pixel. To calculate the total soil loss (*TSL*) for the entire Descoberto River basin and for each watershed within that basin, we multiplied the results by the pixel area (0.09 ha), and then added the values of all the pixels within each watershed to estimate the watershed soil loss.

2.6 Landscape Analysis

We utilized the FRAGSTATS 4.2.1.603 software (McGarigal et al., 2012) to quantify landscape patterns for all 62 watersheds from 1985 to 2017. Our selection of landscape-level metrics was guided by our study objectives, aiming to assess the correlation between landscape fragmentation and soil loss in the study area. Thus, we included metrics that represent the main landscape classes, such as area, edge, core area, aggregation, and diversity patterns, as suggested by Singh et al. (2017), Kumar et al. (2018), and Zhang et al. (2019) (Table 1). These metrics were calculated with an edge size of 100 m (Bircol et al., 2018) and a connection radius of 1000 m (Garcia et al., 2017).

Table 1. Landscape metrics applied in this analysis

Analysis Class	Metrics
Area and Edge Metrics	Largest Patch Index (LPI)
	Total Edge (TE)
	Edge Density (ED)
Core Areas Metrics	Number of Disjunct Core Areas (NDCA)
Aggregation Metrics	Proximity Index Distribution (PROX_MN)
	Number of Patches (NP)
	Patch Density (PD)
	Landscape Shape Index (LSI)
	Landscape Division Index (DIVISION)
	Contagion (CONTAG)
	Splitting Index (SPLIT)
	Interspersion and Juxtaposition Index (IJI)
Diversity	Patch Richness (PR)
	Patch Richness Density (PRD)
	Shannon's Diversity Index (SHDI)
	Shannon's Evenness Index (SHEI)

2.7 Variance and Trend Analysis

The Shapiro-Wilk test indicated a non-normal distribution for both TSL and landscape metrics. Consequently, we used the Kruskal-Wallis test at a significance level of 0.05 to detect differences among watersheds. To identify potential trend shifts in the dataset over the study period, we employed the nonparametric time series trend test proposed by Mann-Kendall. Both variance and trend analyses were conducted using STATA 14.0 software (version 20.0; SPSS Inc., Chicago, IL, USA).

2.8 Principal Component Analysis

The pool of landscape metrics comprised 16 different metrics that reflect the landscape's status. Principal Component Analysis (PCA) is used to objectively identify key factors, reduce dimensionality, and address multicollinearity in the data (Jha et al., 2015). In this analysis, we conducted PCA using STATA® 14.0 software, following three steps: data preparation for the correlation matrix; extraction of common factors; and rotation of the axes relative to these common factors (Sands and Podmore, 2000).

We employed the Varimax Rotation Method to obtain orthogonal principal components (PCs) and selected the main components based on the Kaiser rule (eigenvalues > 1) (Kumar et al., 2018). Additionally, we used the first three components to explain the maximum total data variability, as they showed no correlation and explained over 70% of the total variance (Hair et al., 2009).

To assess the adequacy of the model, we utilized the Kaiser-Meyer-Olkin parameters and Bartlett's sphericity tests. Kaiser-Meyer-Olkin values above 0.6 were considered acceptable, and significant Bartlett's test values were expected to exceed 0.05 (Liu et al., 2016b).

2.9 Geographical and Temporal Weighted Regression

The Geographical and Temporal Weighted Regression (GTWR) model developed by Huang et al. (2010) is expressed as follows:

$$Y_i = \beta_0(u_i, v_i, t_i) + \sum_k \beta_k(u_i, v_i, t_i) X_{ik} + \varepsilon_i \quad (5)$$

Where: (u_i, v_i) = 2D coordinates of the observation *i*; $\beta_0(u_i, v_i, t_i)$ = intercept value; and $\beta_k(u_i, v_i, t_i)$ = *kth* parameter, varying with the 2D coordinates and time (t_i) at the *i* observation.

In this study, *k* was assumed to be 1; *Yi* = the soil loss at the observation *I*; and X_{ik} = the PCs. The estimation of $\beta_k(u_i, v_i, t_i)$ at each space-time observation *i* can be expressed as:

$$\widehat{\beta_k}(u_i, v_i, t_i) = [X^T W(u_i, v_i, t_i) X]^{-1} X^T (u_i, v_i, t_i) Y \quad (6)$$

Where: $W(u_i, v_i, t_i)$ = a spatial temporal weight matrix based on the Euclidean distance and Gaussian distance decay-based functions in space-time domains.

In our analysis, the Euclidean distance was measured in meters and years. The elements of

the spatiotemporal weight matrix were defined as $W_{ij}^{ST} = W_{ij}^{S} \times W_{ij}^{T} \times W_{ij}^{T}$, with the time weighted element between observations i and j; $W_{ij}^{T} = exp\ exp\left(\frac{d_{ij}^2}{h_T^2}\right)$, where: $d_{ij} = \sqrt{(t_i - t_j)^2}$.

Complementarily, h is a non-negative parameter known as bandwidth, which produces a decay of influence with distance, and *dij* is the distance between location *i* and *j*, in this study, measured using a Gaussian Adaptative Kernel and the bandwidth selection criteria, based on the Akaike Information Criterion (AIC).

The goodness fit of the model was assessed by comparing the R^2 and AIC results of the GTWR model with those obtained from the conventional ordinary least square (OLS) model (Du et al., 2018; Ma et al., 2018).

3. Results

3.1 Land Use and Land Cover Changes

We estimated that over 52% of native vegetation in the study area has been converted to other land use types (e.g. pastures, agriculture, water reservoirs, built areas, and forest plantations) by 2017. Most of its territory was covered by a savannah-like vegetation and croplands during the period of analysis. In recent years of our analysis, we observed that savannah and forest formations have slightly increased in the study area, together covering an average of 46% of its territory between 1985 and 2017. Urban areas and rivers/lakes occupied 6.8% and 1.5% of the study area by 2017, respectively (Figure 3).

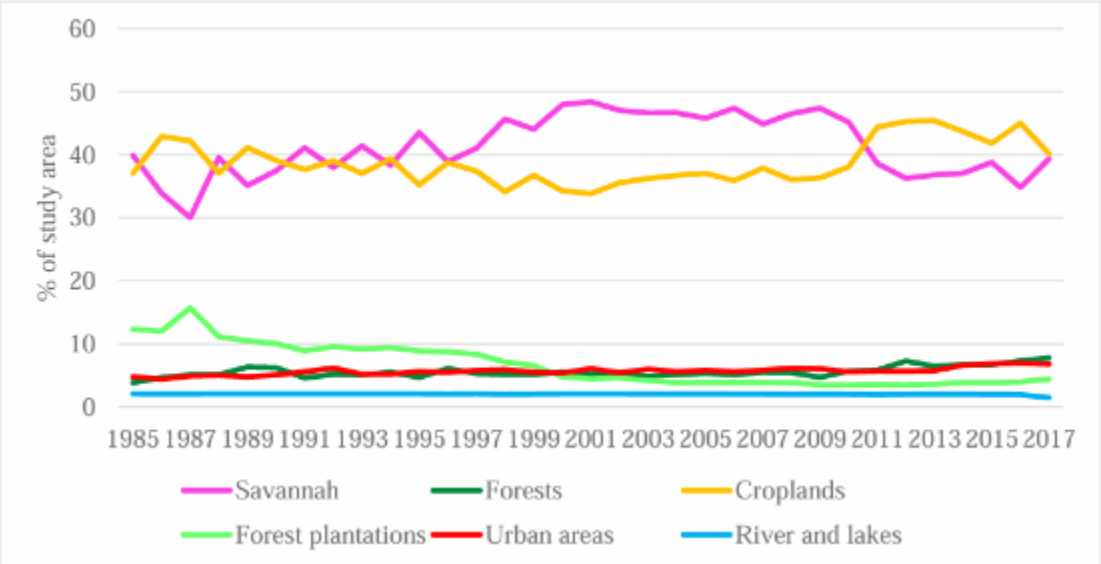

Figure 3. Land use and land cover changes in the Descoberto River basin between 1985 and 2017. Source: Adapted from MapBiomas (2018a)

However, no significant land use changes were observed between 1985 and 2027 in the study

area, although native vegetation has marginally increased from 43.8% in 1985 to 47.2% in 2017, mostly due to vegetation recovery in that region.

3.2 Landscape Metrics

As previously presented, although LULC did not change substantially, the landscape metrics results suggest an increasing landscape fragmentation during the study period. For instance, we estimated an average of 48 patches (NP) ranging from 7 to 136 patches per watershed during the study period. This increased from an average of 40 patches in 1985 to 55 patches in 2017. Similarly, we estimated a patch density (PD) of an average of 12, increasing from 10 to 14 between 1985 and 2017. The largest patch comprised an average of 47% of the watershed landscapes, decreasing from 54% to 41% between 1985 and 2017. The edge density (ED) increased from 60 to 73 between 1985 and 2017, with an average of 71.9 (Table 2).

The aggregation metrics suggest that the landscape in the study area exhibits a certain degree of clumping (CONTAG, average of 52) and a number of land use classes (LSI, average of 5.3). Land use classes are adjacent to each other (IJI, average of 58.5), and the landscape is moderately subdivided (DIVISION, average of 0.7), with a moderate to high number of patches (SPLIT, average of 0.7). The isolation metric PROX (Proximity Index) indicates that patches are moderately distributed in the study area, with an average of 76.

We calculated both Simpson's Heterogeneity Index (SHDI) and Simpson's Evenness Index (SHEI) to assess the distribution of area among patch types for all 62 analyzed watersheds in the study area and period. We estimated an average of 0.95 for SHDI and an average of 0.68 for SHEI among the 62 watersheds. These values suggest an uneven distribution of area among patch types, indicating that certain patch types are more dominant than others in terms of their abundance in the study area. However, the proportional abundances of different patch types are relatively similar across the study area, as suggested by the estimated SHEI value. Additionally, other diversity metrics indicate that there is an average of four land use classes (PR, average of 4.2) with a moderate number of classes in the landscape (PRD, average of 1.95) (Table 2).

Table 2. Statistic summary of the landscape metrics for the 62 watersheds spanning the period from 1985 to 2017

Metric	Mean	Minimum	Maximum	Standard Deviation	CV
NP	48.28	4.00	165.00	29.29	0.61
PD	12.24	2.43	92.59	10.28	0.84
LPI	47.01	14.45	89.82	16.88	0.36
TE	36,648.42	990.00	132,540.00	26,166.12	0.71
ED	71.95	19.14	191.92	22.40	0.31
LSI	5.31	2.16	9.04	1.48	0.28
NDCA	13.79	0.00	49.00	9.13	0.66
PROX_MN	76.19	0.21	469.57	72.39	0.95
CONTAG	51.90	24.84	77.35	8.99	0.17
IJI	58.45	0.00	97.63	15.05	0.26
DIVISION	0.69	0.19	0.92	0.15	0.22
SLIPT	0.69	0.19	0.92	0.15	0.22

PR	4.16	2.00	6.00	0.85	0.20
PRD	1.95	0.20	33.67	4.38	2.25
SHDI	0.95	0.37	1.55	0.19	0.21
SHEI	0.68	0.34	0.97	0.12	0.18

Our landscape metric results indicate that 28 of them exhibited a substantial upward trend in both the number of patches (NP) and patch density (PD) during the study period. Furthermore, 18 of these watersheds showed increasing trends in metrics such as total edge (TE), edge density (ED), and the landscape shape index (LSI) values. Additionally, a significant decreasing trend in the contagion metric (CONTAG) was observed within 24 watersheds between 1985 and 2017. We also noted changes in the landscape concerning patch richness (PR) within 14 watersheds, which showed some decreasing and increasing trends (Figure 4).

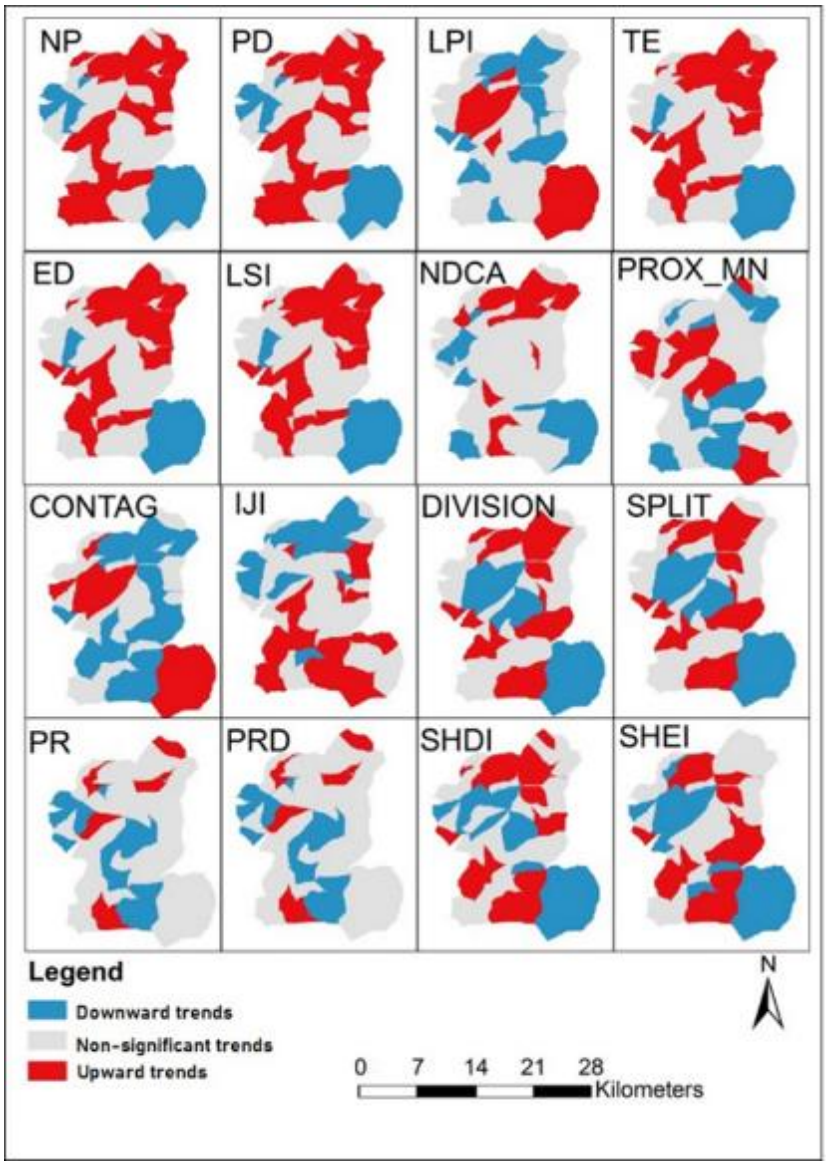

Figure 4. Landscape metrics trend (Mann-Kendall test) observed between 1985 and 2017

In the initial stages, the diversity of patch types increased as various land uses were

introduced during the early phases of human settlement in the study region. This led to the increasing dominance of those newly introduced land uses and a decrease in the richness of patch types.

3.3 Annual Watershed Soil Erosion

The watershed delimitation within the Descoberto River basin has substantially contributed to enhancing the understanding of the intricate relationship between LULC changes and their impact on soil erosion. We estimated an average TSL of 73.3 ± 78.2 (standard deviation) ton ha^{-1} $year^{-1}$ across all 62 analyzed watersheds. Notably, Watershed 38, situated in the central region of the study area, showed the highest TSL at 426.62 ton ha^{-1} $year^{-1}$, while Watershed 52, situated in the southeast, showed the lowest TSL at 0.78 ton ha^{-1} $year^{-1}$ (Figure 5).

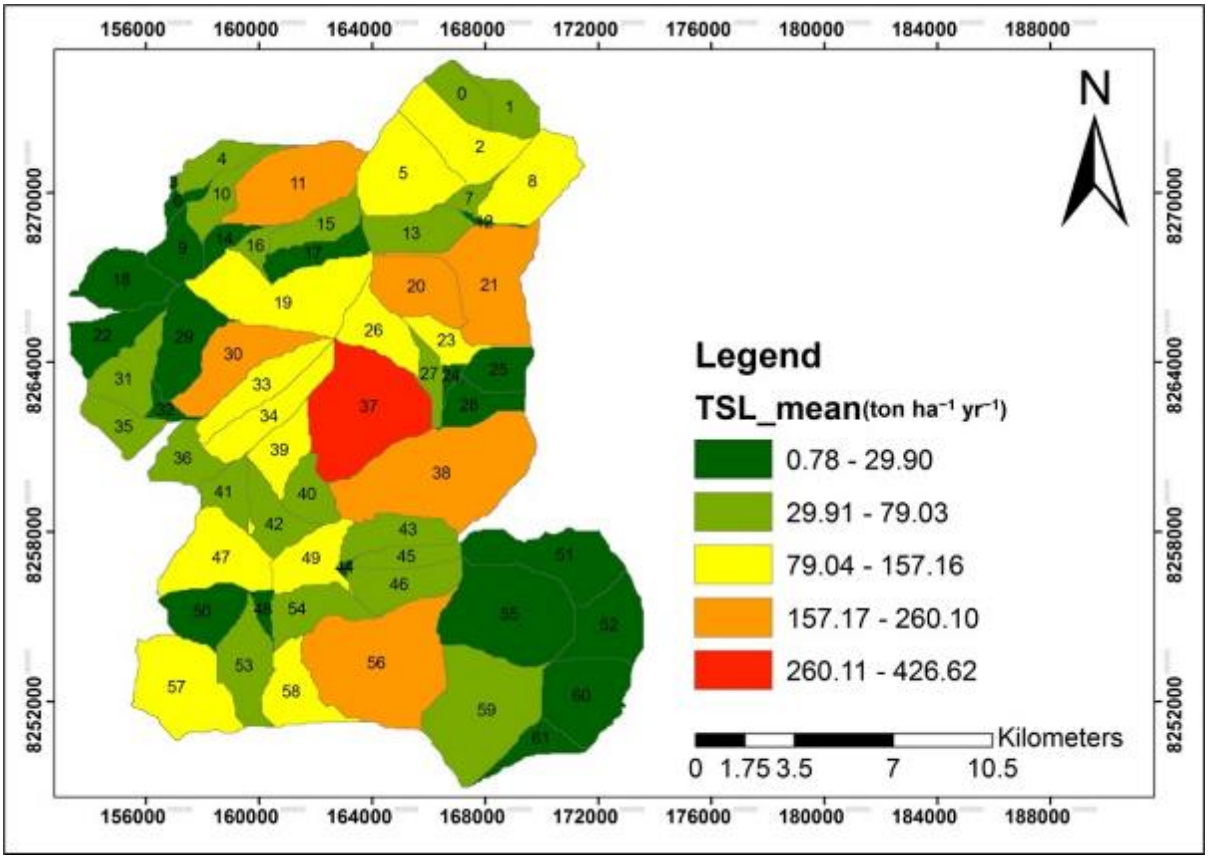

Figure 5. The mean annual Total Soil Loss (TSL) estimated for each watershed spatially located within the Descoberto River basin between 1985 and 2017

Upon analysing our 32-year time-series of TSL dataset, we found that the estimated TSL for the entire Descoberto River basin did not show a statistically significant trend between 1985 and 2017 (Kendall's τ-b = 0.1174; p-value = 0.3446). However, when examining shorter-term intervals, we identified a notable upward trend in TSL between 1985 and 2010 (Kendall's τ-b = 0.5508; p-value = 0.0001), succeeded by a significant downward trend after 2010 (see Figure 4). These findings suggest temporal variations in soil loss dynamics within the basin,

primarily attributed to the recovery of native vegetation since no significant soil management practices were robustly implemented in the study area during the study period.

Among the 62 analyzed watershed, 26 showed no statistically significant changes in TSL during the period of analysis, whereas 20 watersheds exhibited statistically significant decreasing TSL trends, and 16 watersheds displayed statistically significant increasing TSL trends. The estimated TSL values were statistically different among the watersheds (Kruskal-Wallis χ^2 = 1959.314; degrees of freedom = 61; p-value = 0.0001), suggesting that the estimated soil loss depends on the scale of analysis (Chaves, 2010; Ferreira and Ferreira, 2015; Alewell et al., 2019) (Figure 6).

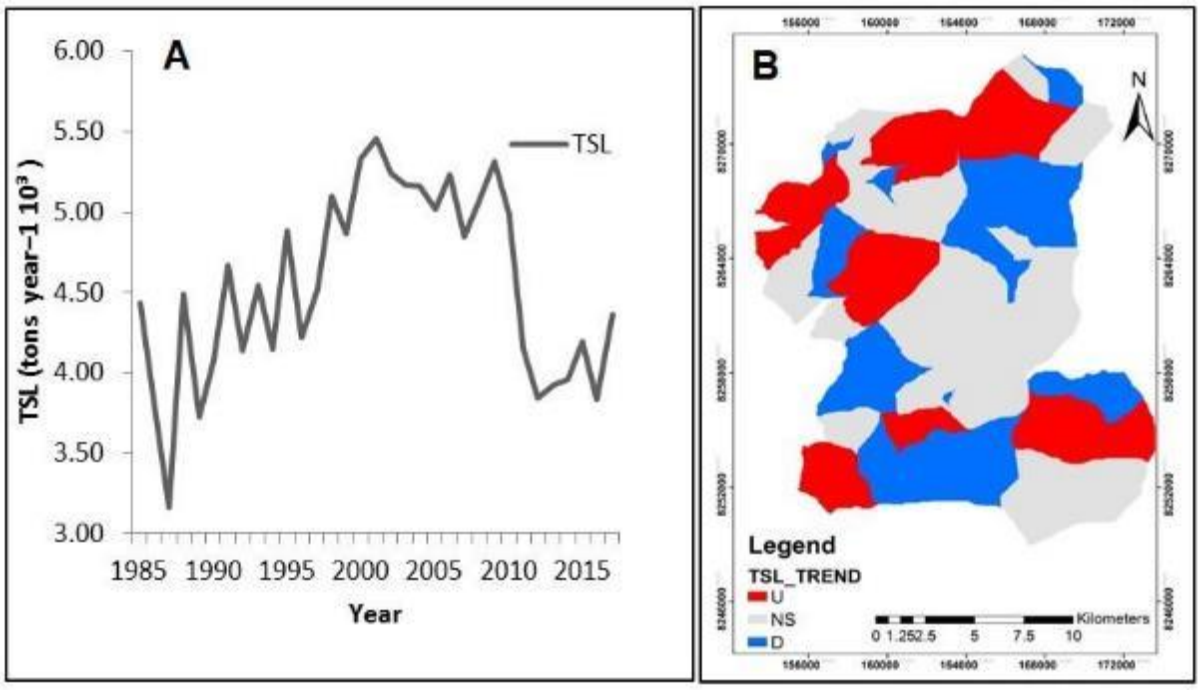

Figure 6. Total soil loss (TSL) in the Descoberto River basin during the period between 1985 and 2017 (A), and TSL trend within the watersheds (B). U= upward trend; NS = not statistically significant; and D = downward trend

We also noted distinct trends in annual precipitation based on datasets from meteorological stations in the region. The Brazlândia meteorological station exhibited a decreasing trend (Kendall's τ-b = −0.3462; p-value = 0.0065), while the Taguatinga meteorological station showed an increasing trend (Kendall's τ-b = 0.2645; p-value = 0.0381). However, for the Descoberto meteorological station, no statistically significant trends were observed in precipitation between 1985 and 2017 (Kendall's τ-b = −0.1785; p-value = 0.1634).

3.4 Principal Component Analysis

The results of the KMO test and Bartlett's sphericity test indicated that the landscape metric dataset was suitable for factor analysis. The overall KMO test yielded a value of 0.685, and the Bartlett's sphericity test was highly significant ($p < 0.000$), suggesting a strong

relationship among the analyzed variables. Following the Kaiser criteria (eigenvalue ≥ 1) and the objective of explaining the maximum variability of the data with no correlation among the components, we extracted and rotated the first three PCs. These three PCs accounted for a total of 76.1% of the data variance.

According to the rotated component matrix (Table 3), the landscape metrics of SHEI, SHDI, CONTAG, DIVISION, SPLIT, and LPI showed the highest loads on PC1 and collectively explained 30.6% of the total data variance.

The loads of landscape metrics of PC extraction were determined using PCA and varimax rotation (Table 3).

Table 3. Statistical results of the principal component analysis of the landscape metrics

Metric	PC 1	PC 2	PC 3
NP	−0.006	0.423	0.021
PD	−0.008	−0.036	0.598
LPI	−0.386	−0.074	−0.011
TE	−0.003	0.423	−0.061
ED	0.151	0.123	0.486
LSI	0.092	0.409	0.016
NDCA	0.024	0.392	−0.105
PROX_MN	−0.082	0.284	−0.166
CONTAG	−0.402	0.101	−0.076
IJI	0.254	−0.266	−0.172
DIVISION	0.385	0.101	0.035
SPLIT	0.376	0.083	0.032
PR	−0.085	0.300	0.136
PRD	−0.086	−0.069	0.546
SHDI	0.310	0.122	0.009
SHEI	0.431	−0.110	−0.097

PC2 explained 29.9% of the data variance and included the following metrics: NP, TE, LSI, and NDCA. NP and LSI measure patch type aggregation or dispersion within a landscape, while TE and NDCA assess the adjacency relationships among patches. In this analysis, PC2 represented the 'dispersion-adjacency' component of the study area's landscape.

PC3 explained 15.6% of the data variance, which was characterized by the loadings of PD (average patch size), PRD (presence of different patch types along the landscape boundary), and ED (patches composed of multiple types). In this case, the PC3 primarily captured attributes related to individual patches.

3.5 Geographically and Temporally Weighted Regression (GTWR)

Our multicollinearity test results showed low variance inflation factor (VIF) values for all variables due to the extraction of principal components (PCs). It indicates that there was no significant multicollinearity among the chosen variables, supported by the observed following VIF values: PC1 = 1.08; PC2 = 1.10; and PC3 = 1.15. These results suggest that the derived PCs from landscape metrics were not strongly correlated with each other. Furthermore, the ordinary least squares (OLS) model showed better statistical results than the

GTWR model in our analysis (Table 4).

Table 4. Comparation between Geographically and Temporally Weighted Regression (GTWR) and Ordinary Least Square (OLS) models.

Model	R^2	AIC
OLS	0.48	22423.33
GTWR	0.87	19665.90

Summary statistics for the GTWR parameters are presented in Table 5. The average coefficients of PC1 (representing aggregation and diversity) and PC3 (representing patch characteristics) were negative.

Table 5. Geographically and Temporally Weighted Regression (GTWR) coefficient's summary statistics

	Mean	Minimum	Maximum	Lower quartile	Median	Upper quartile
Intercept	72.29	−2.92	138.17	50.31	68.67	98.25
PC1	−2.57	−23.36	6.72	−4.96	−1.93	0.69
PC2	20.42	−0.88	47.62	14.52	21.29	26.43
PC3	−6.24	−73.59	60.61	−13.52	−5.71	0.57

The mean of the residuals over time is approximately zero, indicating that the model successfully integrates both space and time (Figure 7). For example, the Watersheds 51, 52, 60, and 61 are located within the Brasília National Forest, whereas the Watersheds 29 and 61 predominantly cover urban areas. Furthermore, the Watersheds 33, 34, and 57 are characterized by croplands and pastures.

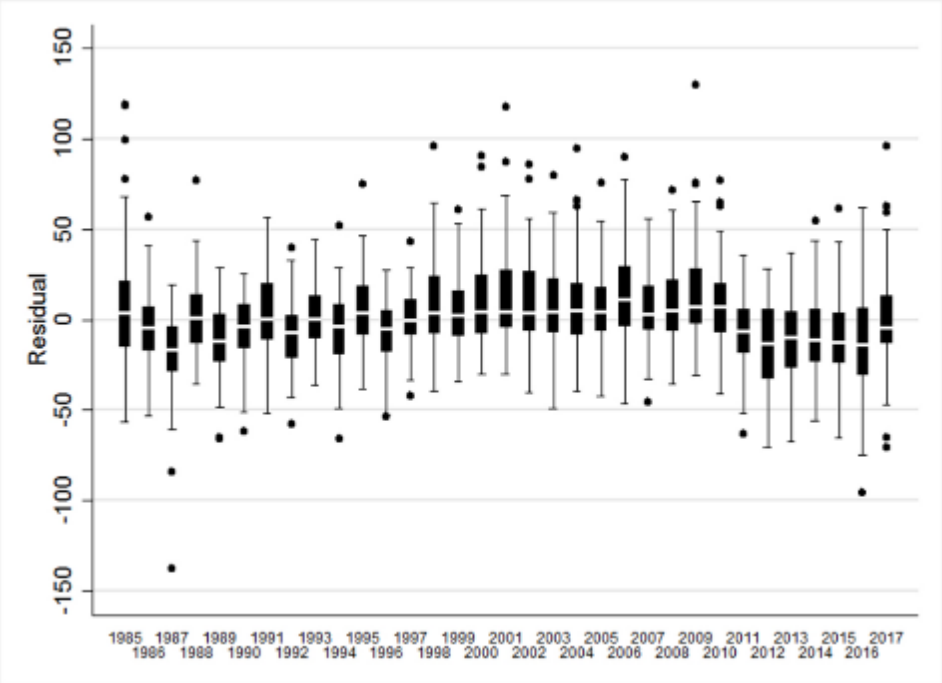

Figure 7. Box plot of the total soil loss (TSL) residuals using the Geographically and Temporally-Weighted Regression (GTWR) model estimated between 1985 and 2017

The dispersion-adjacency coefficients varied across both space and time, as illustrated in Figure 8, reflecting changes in the PC2 coefficient. The most significant changes occurred in 1985 and 1995, predominantly situated in the northeastern and eastern areas of the study region. Conversely, the lowest changes were noted in 2005 and 2017, primarily concentrated in the southeastern and western areas of the study region.

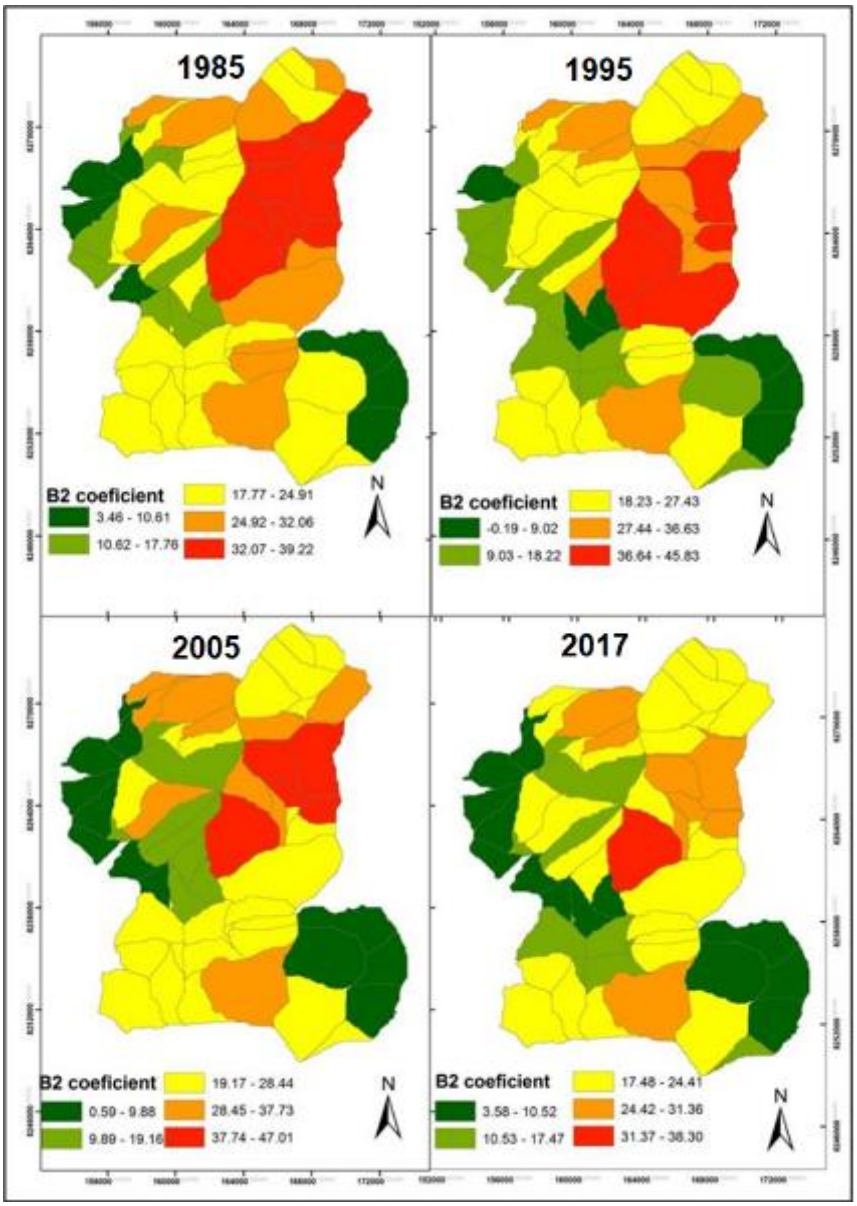

Figure 8. Dispersion-adjacency coefficient spatiotemporal distribution between 1985 and 2017

4. Discussion

4.1 Total Soil Loss

The absence of soil conservation practices has played a crucial role in the increased soil losses observed in 37 watersheds over the study region, which was also observed by Grecchi et al. (2014) and Oliveira et al. (2019) in other study areas in the Cerrado biome. Furthermore, LULC changes have emerged as a significant additional factor driving the overall increase in TSL within our study area. Comparatively, natural landscapes typically show reduced runoff and soil erosion rates in contrast to agricultural lands (Anache et al., 2018). Consequently, watersheds characterized by lower values of the K and LS factors, as well as lower rates of LULC changes, generally exhibit lower TSL values.

By keeping the R, K, L, and S factors constant, our findings highlighted that land use emerges as an important factor shaping soil loss in our study area. Within the Cerrado biome, land use significantly impacts runoff and soil loss rates (Grecchi et al., 2014; Anache et al., 2018). This is particularly true for the predominant Oxisols (referred to as Latosols in the Brazilian Soil Classification System and Ferralsols in the FAO classification), which exhibit high sensitivity to land use changes affecting soil organic matter content (Gmach et al., 2018; James et al., 2019).

The increasing and decreasing trend of TSL observed for 16 and 20 watersheds, respectively, in the study area between 1985 and 2017, indicate that the estimated soil loss is contingent upon the chosen scale of analysis, which can be affected by local factors (Chaves, 2010; Ferreira and Ferreira, 2015; Alewell et al., 2019). For instance, rainfall plays a crucial role in soil erosion by directly influencing TSL (Zhu et al., 2011; Terranova and Gariano, 2015).

Complementarily, disruptions in the organic matter content of Oxisols can compromise their capacity to retain nutrients, diminish structural stability, reduce water holding capability, and ultimately elevate runoff and soil erosion rates (Neufeldt et al., 2002; Gmach et al., 2018; Figuerêdo et al., 2020).

4.2 Landscape Metrics

Our results showed that changes of number of patches (NP) and patch density (PD) are a good indicator of the landscape fragmentation level, which directly affect total edge (TE), number of disjunct core area (NDCA), and edge density (ED) because of the edge effects. This characteristic pattern is also discernible in the landscape shape index (LSI), which is directly affected by the TE. Consequently, an increase in LSI values, as it was observed for our study area, indicates a more irregular landscape shape, ultimately intensifying the complexity of the patch configuration in the landscape.

The decline in patch richness (PR) within the study area's landscape between 1985 and 2017 is primarily resulted from the growing prevalence of introduced anthropogenic land uses in the most recent years of analysis. It directly affects biodiversity and native habitat conservation. It is worth noting that the expansion of croplands and pastures in the study region has been a significant driver of landscape fragmentation. In particular, landscapes dominated by crops tend to be more fragmented compared to those dominated by pastures. A previous study conducted in the Descoberto River basin focusing on identifying land use

conflicts indicated that approximately 40% of the watersheds showed conflicting interests among conservation, agriculture, and urban areas (Nunes and Roig, 2016).

The rapid growth of human activities in the Descoberto River watersheds over the years of our analysis has occurred without proper planning of territorial occupation. The lack of planning has contributed to illegal land occupation and deforestation, which have had detrimental effects on local water resources and soil conservation. Landscape fragmentation, resulting from these activities, directly impacts the nature capacity to provide ecosystem services (Mitchell et al., 2015; Nunes and Roig, 2016).

4.3 Principal Component Analysis

Our observations suggest that some variables (SHEI, SHDI, CONTAG, DIVISION, SPLIT, and LP) were significantly influenced by patterns of aggregation and diversity. This led to the classification of Principal Component 1 (PC1) to represent the "aggregation and diversity" components. In this context, aggregation refers to the tendency of patch types to exhibit spatial clustering or contagiousness, a phenomenon commonly observed in extensive and consolidated distributions.

PC2 comprises the NP, LSI, TE, and NDCA landscape metrics. NP and LSI assess the aggregation and dispersion of patches within a landscape, indicating how scattered a patch type is across the landscape—higher dispersion values suggest greater disaggregation (McGarigal et al., 2012). On the other hand, TE and NDCA metrics focus on adjacency relationships among patches. In this analysis, PC2 represents a 'dispersion-adjacency' component, as it effectively captures landscape patterns related to both patch dispersion and adjacency.

PC3 primarily captured characteristics of individual patch-related landscape metrics, such as PD, PRD, and ED. Specifically, PD represents the average patch size, PRD signifies the presence of diverse patch types along the landscape boundary, and ED highlights scenarios where a patch comprises multiple patch types. In this context, PC3 primarily captured attributes related to individual patches.

We also observed that our study area covers several watershed territories, which highlights the distinct and valuable nature of the metrics ED and TE for this analysis. Due to their substantial explanatory power, we deemed that the three principal components (PC1, PC2, and PC3) are suitable as independent variables to be included in the GTWR model. These components collectively account for 76.1% of the data variance, surpassing the 70% threshold (Hair et al., 2009).

4.4 Geographically and Temporally Weighted Regression

Compared to the conventional OLS model (as presented in Table 4), the GTWR model demonstrated superior statistical performance. It exhibited enhanced explanatory capability by incorporating both spatial and temporal information into the model, which aligns well with findings from prior research (Ma et al., 2018). Previous studies consistently indicate that the GTWR model excels in explaining spatially dependent environmental phenomena by

considering the inherent spatial relationships and patterns in the data (Chu et al., 2018; Du et al., 2018; Li et al., 2020).

The negative average GTWR coefficients for PC1 and PC3 suggest that watersheds with higher scores in these components tend to have lower TSL. These components reflect landscape fragmentation, with higher scores indicating less diversity and more spatial aggregation, which is associated with lower TSL.

Conversely, higher values of PC2, representing dispersion-adjacency, were positively correlated with high TSL. Watersheds with higher PC2 scores, indicating greater patch dispersion and adjacency, tend to have higher TSL.

The variations in the range of the residuals can be attributed to changes in land use within the study basin. The diverse land use compositions across the watersheds contribute to these observed variations in the residuals. The changes seen in the residuals after 2010, as depicted in Figure 3, are likely due to a decreasing trend in soil loss within the watersheds. This suggests a recovery of Cerrado vegetation by 2015 in most of the studied watersheds compared to previous years. For instance, by 2015, the Cerrado area had increased by 10.5%, cropped area had decreased by 6.3%, and urbanized area had increased by 43.6%. Natural regeneration in the Cerrado biome contributes to improving soil conditions by enhancing infiltration, reducing surface runoff, and lowering erosion rates (Falcão et al., 2020).

We observed that, simultaneously, land use changes are influenced by various temporal and spatial factors, such as economic opportunities, soil type, streams, and roads (Liu et al., 2016a; Garcia et al., 2017; Zimbres et al., 2018). These factors, crucial to the study area, exacerbate fragmentation and soil erosion processes, underscoring the need to adopt soil erosion management techniques and soil conservation measures.

This study provides a comprehensive analysis and information on the effects of LULC changes on landscape fragmentation and soil erosion in the Descoberto River basin. It illustrates the spatiotemporal dynamics of landscape fragmentation and soil loss in the study area, both as a whole and on an individual watershed basis. The findings have the potential to be applied in supporting definition of public policies related to land use and soil management to mitigate deforestation impacts, thereby enhancing the production of ecosystem services, including water yield and infiltration.

5. Conclusions

The land use and soil management factor (CP) have undergone changes over time in the study area. The absence of proper soil management practices has emerged as the primary driving force behind soil loss. However, a comprehensive analysis is necessary to fully grasp all the factors influencing soil losses in the study region, including economic opportunities, soil types, streams, and the road network.

The use of the PCA reduction technique identified three key landscape components (aggregation/diversity, dispersion/adjacency, and patchiness) that represent different aspects related to soil erosion in the study area. TSL increased as the dispersion-adjacency factor

increased, as this landscape metric is positively associated with the level of fragmentation and soil erosion in the Descoberto River basin. Additionally, lower levels of TSL were directly linked to less diverse and more aggregated landscapes in the study area.

The trends of TSL resulting from landscape fragmentation were non-linear, suggesting that discretized and spatial-temporal models (such as the GTWR) were better suited for analyzing water and soil resources in the study area. These modeling results indicate a decreasing trend in soil loss rates by 2015, compared to previous years, likely due to recent native vegetation recovery.

Lastly, we recommend the use of GTWR to assist stakeholders in identifying priority areas for implementing soil and water conservation measures. Changes in the provision of these ecological services directly impact water reservoirs and agricultural production in the Descoberto River basin, Federal District of Brazil.

Authors contributions

Dr. ANA PAULA CAMELO and Dr. ERALDO MATRICARDI were responsible for the research design, Dr. ANA PAULA CAMELO and Dr. KEILA SANCHES were responsible for data collection, Dr. ANA PAULA CAMELO, Dr. KEILA SANCHES, and Dr. EDER PEREIRA MIGUEL data preparation and analysis. Dr. ANA PAULA CAMELO and Dr. KEILA SANCHES provided some of the field data and supplied technical support. Dr. ANA PAULA CAMELO, Dr. KEILA SANCHES, Dr. EDER PEREIRA MIGUEL, Dr. EDSON EIJY SANO, and Dr. ALVARO NOGUEIRA DE SOUZA drafted the manuscript. Dr. ANA PAULA CAMELO, Dr. ERALDO MATRICARDI and Dr. EDSON EYJI SANO were responsible for writing—review and final editing. All authors have read and agreed to the published version of the manuscript.

Acknowledgements

We would like to thank every team and faculty members who took the time to participate in this study. We also sincerely thank the editorial team of this scientific journal for their work, support, and contributions in the final version of this manuscript.

Funding

This work was financially supported in part by the National Council for Scientific and Technological Development (CNPq), Grants n. 401892/2021-2 and n. 311155/2020-0.

Competing interests

The authors declare that they have no known competing financial interests or personal relationships that could have appeared to influence the work reported in this paper.

Informed consent

Obtained.

Ethics approval

The Publication Ethics Committee of the Macrothink Institute.

The journal's policies adhere to the Core Practices established by the Committee on Publication Ethics (COPE).

Provenance and peer review

Not commissioned, externally double-blind peer reviewed.

Data availability statement

The data that support the findings of this study are available on request from the corresponding author. The data are not publicly available due to privacy or ethical restrictions.

Data sharing statement

No additional data are available.

Open access

Copyrights

References

Alewell, C., Borrelli, P., Meusburger, K., & Panagos, P. (2019). Using the USLE: Chances, challenges and limitations of soil erosion modelling. *International Soil and Water Conservation Research, 7*(3), 203-225. https://doi.org/10.1016/j.iswcr.2019.05.004.

Anache, J. A. A., Flanagan, D. C., Srivastava, A., & Wendland, E. C. (2018). Land use and climate change impacts on runoff and soil erosion at the hillslope scale in the Brazilian Cerrado. *Science of the Total Environment, 622-623*, 140-151. https://doi.org/10.1016/j.scitotenv.2017.11.257.

Benavidez, R., Jackson, B., Maxwell, D., & Norton, K. (2018). A review of the (Revised) Universal Soil Loss Equation ((R) USLE): with a view to increasing its global applicability and improving soil loss estimates. *Hydrology and Earth System Sciences, 22*(11), 6059-6086. https://doi.org/1010.5194/hess-22-6059-2018

Bera, A. (2017). Assessment of soil loss by universal soil loss equation (USLE) model using GIS techniques: A case study of Gumti River Basin, Tripura, India. *Modeling Earth Systems and Environment, 3*(1), 29. https://doi.org/10.1007/s40808-017-0289-9

Bertoni, J., & Lombardi Neto, F. (1999). *Conservação do Solo,* Icone, São Paulo, SP, Brazil (4th ed.).

Bircol, G. A. C., Souza, M. P., Fontes, A. T., Chiarello, A. G., & Ranieri, V. E. L. (2018). Planning by the rules: A fair chance for the environment in a land-use conflict area. *Land Use Policy, 76*, 103-112. https://doi.org/10.1016/j.landusepol.2018.04.038

Borrelli, P., Robinson, D. A., Panagos, P., Lugato, E., Yang, J. E., Alewell, C., Wuepper, D., Montanarella, L., & Ballabio, C. (2020). Land use and climate change impacts on global soil erosion by water (2015-2070). *Proceedings of the National Academy of Sciences, 117*(36), 21994-22001. https://doi.org/10.1073/pnas.2001403117

Chaves, H. M. L. (2010). Incertezas na predição da erosão com a USLE: Impactos e mitigação. *Revista Brasileira de Ciência do Solo, 34*, 2021-2029.

Chu, H.-J., Kong, S.-J., & Chang, C.-H. (2018). Spatio-temporal water quality mapping from satellite images using geographically and temporally weighted regression. *International Journal of Applied Earth Observation and Geoinformation, 65*, 1-11. https://doi.org/10.1016/j.jag.2017.10.001

CODEPLAN (2020). *Atlas do Distrito Federal.* [Online] Available: https://www.codeplan.df.gov.br/wp-content/uploads/2018/05/Atlas-do-Distrito-Federal-2020-Apresenta%C3%A7%C3%A3o-e-Cap%C3%ADtulo-1.pdf

Cui, L., Li, R., Zhang, Y., Meng, Y., Zhao, Y., & Fu, H. (2019). A geographically and temporally weighted regression model for assessing intra-urban variability of volatile organic compounds (VOCs) in Yangpu district, Shanghai. *Atmospheric Environment, 213*, 746-756. https://doi.org/10.1016/j.atmosenv.2019.06.052

Du, Z., Wu, S., Zhang, F., Liu, R., & Zhou, Y. (2018). Extending geographically and temporally weighted regression to account for both spatiotemporal heterogeneity and seasonal variations in coastal seas. *Ecological Informatics, 43*, 185-199. https://doi.org/10.1016/j.ecoinf.2017.12.005

Falcão, K. S., Panachuki, E., Monteiro, F. N., Menezes, R. S., Rodrigues, D. B. B., Sone, J. S., & Oliveira, P. T. S. (2020). Surface runoff and soil erosion in a natural regeneration area of the Brazilian Cerrado. *International Soil and Water Conservation Research, 8*(2), 124-130. https://doi.org/10.1016/j.iswcr.2020.04.004.

Ferreira, L. M., & Ferreira, A. G. (2015). Aplicação de um modelo de erosão hídrica do solo à escala da unidade de intervenção florestal com a utilização de um Sistema de Informação Geográfica. *Revista de Ciências Agrárias, 38*, 587-597. https://doi.org/10.19084/RCA15141

Ferreira, K.C.D., Lopes, F. B., Andrade, E. M., Meireles, A. C. M., & Silva, G. S. (2015). Adaptação do índice de qualidade de água da National Sanitation Foundation ao semiárido brasileiro. *Revista Ciência Agronômica, 46*(2), 277-286. https://doi.org/10.5935/1806-6690.20150007

Figuerêdo, K. S., Pereira, M. T. J., Nick, C., Silva, I. R., & Oliveira, T. S. (2020). Long-term

changes in organic matter stocks and quality in an Oxisol under intensive vegetable cultivation. *Catena, 188*, 104442. https://doi.org/10.1016/j.catena.2019.104442

Fotheringham, A. S., Brunsdon, C., & Charlton, M. (2002). *Geographically Weighted Regression: The Analysis of Spatially Varying Relationships.* John Wiley & Sons, West Sussex, England.

Gao, J., & Wang, H. (2019). Temporal analysis on quantitative attribution of karst soil erosion: A case study of a peak-cluster depression basin in Southwest China. *Catena, 172*, 369-377. https://doi.org/10.1016/j.catena.2018.08.035

Garcia, A. S., Sawakuchi, H. O., Ferreira, M. E., & Ballester, M. V. R. (2017). Landscape changes in a neotropical forest-savanna ecotone zone in central Brazil: The role of protected areas in the maintenance of native vegetation. *Journal of Environmental Management, 187*, 16-23. Available: https://doi.org/10.1016/j.jenvman.2016.11.010

Garrett, R. D., Koh, I., Lambin, E. F., Waroux, Y. P., Kastens, J. H., & Brown, J. C. (2018). Intensification in agriculture-forest frontiers: Land use responses to development and conservation policies in Brazil. *Global Environmental Change, 53*, 233-243. https://doi.org/10.1016/j.gloenvcha.2018.09.011

Gmach, M.-R., Dias, B. O., Silva, C. A., Nóbrega, J. C. A., Lustosa-Filho, J. F., & Siqueira-Neto, M. (2018). Soil organic matter dynamics and land-use change on Oxisols in the Cerrado, Brazil. *Geoderma Regional, 14*, e00178. https://doi.org/10.1016/j.geodrs.2018.e00178

Grecchi, R. C., Gwyn, Q. H. J., Bénié, G. B., Formaggio, A. R., & Fahl, F. C. (2014). Land use and land cover changes in the Brazilian Cerrado: A multidisciplinary approach to assess the impacts of agricultural expansion. *Applied Geography, 55*, 300-312. https://doi.org/10.1016/j.apgeog.2014.09.014

Hair, J. F., Black, W. C., Babin, B. J., Anderson, R. E., & Tatham, R. L. (2009). *Análise Multivariada de Dados* (6th ed.). Bookman Editora, Porto Alegre, RS, Brazil.

Hrachowitz, M., Savenije, H. H. G., Blöschl, G., McDonnell, J. J., Sivapalan, M., ... Pomeroy, J. W. (2013). A decade of predictions in ungauged basins (PUB)—a review. *Hydrological Sciences Journal, 58*(6), 1198-1255. https://doi.org/10.1080/02626667.2013.803183

Hu, M., Li, Z., Yuan, M., Fan, C., & Xia, B. (2019). Spatial differentiation of ecological security and differentiated management of ecological conservation in the Pearl River Delta, China. *Ecological Indicators, 104*, 439-448. https://doi.org/10.1016/j.ecolind.2019.04.081

Huang, B., Wu, B., & Barry, M. (2010). Geographically and temporally weighted regression for modeling spatio-temporal variation in house prices. *International Journal of Geographical Information Science, 24*(3), 383-401. https://doi.org/10.1080/13658810802672469

Hurtt, G. C., Chini, L., Sahajpal, R., Frolking, S., Bodirsky, B. L., … Calvin, K. (2020). Harmonization of global land use change and management for the period 850–2100 (LUH2)

for CMIP6. *Geoscientific Model Development, 13*(11), 5425-5464. https://doi.org/10.5194/gmd-13-5425-2020

James, J. N., Gross, C. D., Dwivedi, P., Myers, T., Santos, F., Bernardi, R., Faria, M. F., Guerrini, I. A., Harrison, R., & Butman, D. (2019). Land use change alters the radiocarbon age and composition of soil and water-soluble organic matter in the Brazilian Cerrado. *Geoderma, 345*, 38-50. https://doi.org/10.1016/j.geoderma.2019.03.019

Jha, D. K., Devi, M. P., Vidyalakshmi, R., Brindha, B., Vinithkumar, N. V., & Kirubagaran, R. (2015). Water quality assessment using water quality index and geographical information system methods in the coastal waters of Andaman Sea, India. *Marine Pollution Bulletin, 100*(1), 555-561. https://doi.org/10.1016/j.marpolbul.2015.08.032

Jusys, T. (2016). Fundamental causes and spatial heterogeneity of deforestation in Legal Amazon. *Applied Geography, 75*, 188-199. https://doi.org/10.1016/j.apgeog.2016.08.015

Kassawmar, T., Eckert, S., Hurni, K., Zeleke, G., & Hurni, H. (2018). Reducing landscape heterogeneity for improved land use and land cover (LULC) classification across the large and complex Ethiopian highlands. *Geocarto International, 33*(1), 53-69. https://doi.org/10.1080/10106049.2016.1222637

Kumar, M., Denis, D. M., Singh, S. K., Szabó, S., & Suryavanshi, S. (2018). Landscape metrics for assessment of land cover change and fragmentation of a heterogeneous watershed. *Remote Sensing Applications: Society and Environment, 10*, 224-233. https://doi.org/10.1016/j.rsase.2018.04.002

Ledda, A., & Montis, A. (2019). Infrastructural landscape fragmentation versus occlusion: A sensitivity analysis. *Land Use Policy, 83*, 523-531. https://doi.org/10.1016/j.landusepol.2019.02.035

Li, R., Cui, L., Fu, H., Meng, Y., Li, J., & Guo, J. (2020). Estimating high-resolution PM1 concentration from Himawari-8 combining extreme gradient boosting-geographically and temporally weighted regression (XGBoost-GTWR). *Atmospheric Environment, 229,* 117434. https://doi.org/10.1016/j.atmosenv.2020.117434

Liao, C., Tesfa, T., Duan, Z., & Leung, L. R. (2020). Watershed delineation on a hexagonal mesh grid. *Environmental Modelling & Software, 128*, 104702. https://doi.org/10.1016/j.envsoft.2020.104702

Liu, Y., Feng, Y., Zhao, Z., Zhang, Q., & Su, S. (2016a). Socioeconomic drivers of forest loss and fragmentation: A comparison between different land use planning schemes and policy implications. *Land Use Policy, 54*, 58-68. https://doi.org/10.1016/j.landusepol.2016.01.016

Liu, Y., Wei, X., Li, P., & Li, Q. (2016b). Sensitivity of correlation structure of class- and landscape-level metrics in three diverse regions. *Ecological Indicators, 64*, 9-19. https://doi.org/10.1016/j.ecolind.2015.12.021.

Lopes, J. A. A., Bias, E. S., & Ribeiro, R. J. C. (2009). Aplicação da USLE para avaliação de

perdas de solo no município de Águas Lindas de Goiás-GO. *Geografia, 34*(2), 347-369.

Ma, X., Zhang, J., Ding, C., & Wang, Y. (2018). A geographically and temporally weighted regression model to explore the spatiotemporal influence of built environment on transit ridership. *Computers, Environment and Urban Systems, 70,* 113-124..https://doi.org/10.1016/j.compenvurbsys.2018.03.001

Mannigel, A. R., Passos, M., Moreti, D., & Medeiros, L. R. (2002). Fator erodibilidade e tolerância de perda dos solos do Estado de São Paulo. *Acta Scientiarum. Agronomy, 24*, 1335-1340. https://doi.org/10.4025/actasciagron.v24i0.2374

MapBiomas (2018a). *Coleção 3.0 da Série Anual de Mapas de Cobertura e Uso de Solo do Brasil*. [Online] Available: https://brasil.mapbiomas.org/map/colecao-3/

MapBiomas (2018b). *MapBiomas General "Handbook" - Algorithm Theoretical Basis Document (ATBD)*. [Online] Available: https://storage.googleapis.com/mapbiomas/base-de-dados/metodologia/colecao-3_0/1-ATBD-Collection-3-version-1.pdf

McGarigal, K., Cushman, S. A., & Ene, E. (2012). *FRAGSTATS v4: Spatial Pattern Analysis Program for Categorical and Continuous Maps* (4th ed.). University of Massachusetts, Amherst, USA.

Mitchell, M. G. E., Suarez-Castro, A. F., Martinez-Harms, M., Maron, M., McAlpine, C., Gaston, K. J., Johansen, K., & Rhodes, J. R. (2015). Reframing landscape fragmentation's effects on ecosystem services. *Trends in Ecology & Evolution, 30*(4), 190-198. https://doi.org/10.1016/j.tree.2015.01.011

NASA- National Aeronautics and Space Administration. (2023). *NASADEM Merged DEM Global 1 arc second V001*. [Online] Available: https://cmr.earthdata.nasa.gov/search/concepts/C1546314043-LPDAAC_ECS.html

Neufeldt, H., Resck, D. V. S., & Ayarza, M. A. (2002). Texture and land-use effects on soil organic matter in Cerrado Oxisols, Central Brazil. *Geoderma, 107*(3), 151-164. https://doi.org/10.1016/S0016-7061(01)00145-8

Nunes, J. F., & Roig, H. L. (2016). Modelagem dos conflitos de uso e ocupação do solo como ferramenta para o planejamento territorial: O caso da bacia do alto curso do rio Descoberto DF/GO. *Revista Brasileira de Cartografia, 68*(7), 1285-1301.

Nyikadzino, B., Chitakira, M., & Muchuru, S. (2020). Rainfall and runoff trend analysis in the Limpopo river basin using the Mann Kendall statistic. *Physics and Chemistry of the Earth, Parts A/B/C, 117,* 102870. https://doi.org/10.1016/j.pce.2020.102870

Oliveira, V. A., Mello, C. R., Beskow, S., Viola, M. R., & Srinivasan, R. (2019). Modeling the effects of climate change on hydrology and sediment load in a headwater basin in the Brazilian Cerrado biome. *Ecological Engineering, 133,* 20-31. https://doi.org/10.1016/j.ecoleng.2019.04.021

Ouyang, W., Skidmore, A. K., Hao, F., & Wang, T. (2010). Soil erosion dynamics response to landscape pattern. *Science of the Total Environment, 408*(6), 1358-1366. https://doi.org/10.1016/j.scitotenv.2009.10.062

Qi, S. S., Hao, F. H., Ouyang, W., & Cheng, H. G. (2012). Characterizing landscape and soil erosion dynamics under pipeline interventions in Southwest China. *Procedia Environmental Sciences, 13*, 1863-1871. https://doi.org/10.1016/j.proenv.2012.01.180

Queiroz, A. C. M., Rabello, A. M., Braga, D. L., Santiago, G. S., Zurlo, L. F., Philpott, S. M., Ribas, C. R. (2020). Cerrado vegetation types determine how land use impacts ant biodiversity. *Biodiversity and Conservation, 29*(6), 2017-2034. https://doi.org/10.1007/s10531-017-1379-8

Reatto, A., Martins, E. S., Cardoso, E. A., Spera, S. T., Carvalho Júnior, O. A., Guimarães, R., Silva, A. V., & Farias, M. F. R. (2003). *Levantamento de reconhecimento de solos de alta intensidade do alto curso do Rio Descoberto, DF/GO, escala 1:100.000*. Embrapa Cerrados, Planaltina, DF. Boletim de Pesquisa e Desenvolvimento, 92.

Sands, G. R., & Podmore, T. H. (2000). A generalized environmental sustainability index for agricultural systems. *Agriculture, Ecosystems & Environment, 79*(1), 29-41. https://doi.org/10.1016/S0167-8809(99)00147-4

Schwieder, M., Leitão, P. J., Bustamante, M. M. C., Ferreira, L. G., Rabe, A., & Hostert, P. (2016). Mapping Brazilian savanna vegetation gradients with Landsat time series. *International Journal of Applied Earth Observation and Geoinformation, 52*, 361-370. https://doi.org/10.1016/j.jag.2016.06.019

SEDUH (2019). *Geoportal de dados espaciais. Infraestrutura de Dados Espaciais - IDE/DF.* [Online] Available: https://www.geoportal.seduh.df.gov.br/mapa/

Silva, A. M., & Alvares, C. A. (2007). Levantamento de informações e estruturação de um banco dados sobre a erodibilidade de classes de solos no estado de São Paulo. *Geociências (São Paulo), 24*(1), 33-41.

Singh, S. K., Srivastava, P. K., Szabó, S., Petropoulos, G. P., Gupta, M., & Islam, T. (2017). Landscape transform and spatial metrics for mapping spatiotemporal land cover dynamics using Earth Observation data-sets. *Geocarto International, 32*(2), 113-127. https://doi.org/10.1080/10106049.2015.1130084

Soares-Filho, B., Rodrigues, H., & Follador, M. (2013). A hybrid analytical-heuristic method for calibrating land-use change models. *Environmental Modelling & Software, 43*, 80-87. https://doi.org/10.1016/j.envsoft.2013.01.010

Tadesse, L., Suryabhagavan, K. V., Sridhar, G., & Legesse, G. (2017). Land use and land cover changes and soil erosion in Yezat Watershed, North Western Ethiopia. *International Soil and Water Conservation Research, 5*(2), 85-94. https://doi.org/10.1016/j.iswcr.2017.05.004

Terranova, O. G., & Gariano, S. L. (2015). Regional investigation on seasonality of erosivity

in the Mediterranean environment. *Environmental Earth Sciences, 73*(1), 311-324. https://doi.org/10.1007/s12665-014-3426-z

Tiwari, S., Jha, S. K., & Sivakumar, B. (2019). Reconstruction of daily rainfall data using the concepts of networks: Accounting for spatial connections in neighborhood selection. *Journal of Hydrology, 579*, 124185. https://doi.org/10.1016/j.jhydrol.2019.124185

Trabaquini, K., Galvão, L. S., Formaggio, A. R., & Aragão, L. E. O. C. (2017). Soil, land use time, and sustainable intensification of agriculture in the Brazilian Cerrado region. *Environmental Monitoring and Assessment, 189*(2), 70. https://doi.org/10.1007/s10661-017-5787-8

Wischmeier, W. H., & Mannering, J. V. (1969). Relation of soil properties to its erodibility. *Soil Science Society of America Journal, 33*(1), 131-137. https://doi.org/10.2136/sssaj1969.03615995003300010035x

Wischmeier, W. H., & Smith, D. D. (1978). *Predicting Rainfall Erosion Losses.* A Guide to Conservation Planning. USDA, Washington, DC, Agriculture Handbook no. 537.

Wuepper, D., Borrelli, P., & Finger, R. (2020). Countries and the global rate of soil erosion. *Nature Sustainability, 3*(1), 51-55. https://doi.org/10.1038/s41893-019-0438-4

Zhang, J., Li, S., Dong, R., Jiang, C., & Ni, M. (2019). Influences of land use metrics at multi-spatial scales on seasonal water quality: A case study of river systems in the Three Gorges Reservoir Area, China. *Journal of Cleaner Production, 206*, 76-85. https://doi.org/10.1016/j.jclepro.2018.09.179

Zhu, Q., Chen, X., Fan, Q., Jin, H., & Li, J. (2011). A new procedure to estimate the rainfall erosivity factor based on Tropical Rainfall Measuring Mission (TRMM) data. *Science China Technological Sciences, 54*(9), 2437. https://doi.org/10.1007/s11431-011-4468-z

Zimbres, B., Machado, R. B., & Peres, C. A. (2018). Anthropogenic drivers of headwater and riparian forest loss and degradation in a highly fragmented southern Amazonian landscape. *Land Use Policy, 72*, 354-363. https://doi.org/10.1016/j.landusepol.2017.12.062

Copyright Disclaimer